ARTICLE NO. 78-418

Development of a Liquid-Trap Heat Pipe Thermal Diode

M. Groll,* W.D. Münzel,† W. Supper‡
Institut für Kernenergetik und Energiesysteme (IKE), Universität Stuttgart, Stuttgart, Germany
and
C.J. Savage§
European Space Research and Technology Centre (ESTEC), Noordwijk, The Netherlands

An all-aluminum axial-groove liquid-trap heat pipe diode, 470 mm long and 10 mm o.d., has been developed with a forward-mode performance of nearly 90 Wm, when ammonia is used as the working fluid at 20°C. The diode is bendable, of simple design, and of reliable performance. A mathematical model, based on an energy balance for evaporator and trap, has been developed for predicting the transient shutdown of the diode. Theroretical predictions and experimental results are in good agreement. The time for complete shutdown of the diode is on the order of 20 min. The respective shutdown energy is about 4 Wh. A reverse-mode heat flow of about 1.5 W has been measured. Thereby, a turndown ratio of about 300 has been established.

Introduction

HEAT pipe thermal diodes and thermal switches find growing interest for various space applications. For example, a thermal diode may protect a component from overheating during critical periods such as prelaunch operation (especially for cryogenic temperature applications), orientation maneuvers, and re-entry. A thermal switch could be used to transport heat from a component to one of several heat sinks selected at will. Various diode and switch techniques have been discussed in the literature and some of them have been investigated experimentally.[1-8]

The development work described in this paper was undertaken with regard to a potential near-room-temperature application of a thermal diode for Spacelab. The work comprises a comparison of various shutdown techniques, design and development of a thermal diode heat pipe, prediction of forward-mode and transient shutdown performance, and testing of the diode heat pipe.

Diode Design

The overall heat pipe geometry is defined by the following data:

Total length including liquid reservoir or trap	≤500 mm
Evaporator length	100 mm
Adiabatic section length	200 mm
Condenser length	100 mm
Liquid reservoir or trap length	≤100 mm
Heat pipe outer diameter	10 mm
Trap or reservoir outer diameter	≤25 mm

A forward-mode heat transport capability of 50 Wm at 20°C operating temperature and for horizontal operation is required. For the given geometrical data this corresponds to a maximum performance of 167 W. However, the reverse-mode heat flow should be as small as possible—less than 10 W for the potential application. Various heat pipe concepts potentially able to meet these requirements have been compared with respect to their forward- and reverse-mode performance. The three concepts selected for a more detailed comparison are (Fig. 1):

1) All-aluminum axial-groove heat pipe employing the liquid trap technique.

2) All-stainless-steel arterial heat pipe ("eight-shaped" artery) employing either the liquid blockage or trap technique.

3) All-stainless-steel arterial heat pipe ("modular" artery) employing either the liquid blockage or trap technique.

For all diode heat pipes, ammonia has been selected as the working fluid.

The diode concepts have been compared on the basis of the following criteria: 1) thermal performance in the forward-mode operation, 2) thermal performance in the reverse-mode operation, especially turndown ratio and shutdown energy, 3) bendability without performance degradation, 4) 1-g testing capability, 5) mass and volume requirements, and 6) reliability and available experience.

The comparison, based on the same outer diameter of 10 mm, showed a distinctive weight advantage of the axial groove design (90 g vs 145 g for the eight-shaped artery design and 200 g for the modular artery design).

The 1-g testing capability of the axial-groove heat pipe was rated as sufficient, though the arterial heat pipes having triangular circumferential grooves or one layer of screen at the wall as secondary wick are superior (Table 1).

The reverse-mode heat flow by conduction in the diode wall for an assumed temperature difference of 40 K between evaporator and condenser is shown in Table 2 for $L = 20$ cm.

The theoretical shutdown energy (Table 3) was calculated using the equation $Q_{SD} = m_l \cdot h_{fg}$, with m_l the amount of liquid to be evaporated from the heat pipe into the trap (then $m_l = m_{l,\,\mathrm{wick}}$, liquid saturating the wick) or from the reservoir into the heat pipe (then $m_l = m_{\mathrm{ev+ad}}$, liquid in the reservoir, assumed to block the vapor space of evaporator and adiabatic section).

The all-stainless-steel designs have a considerably smaller reverse-mode heat flow which makes them especially promising for cryogenic temperature applications. The theoretical shutdown energies for the axial groove and eight-shaped artery liquid trap designs are about the same and somewhat smaller than for the modular artery liquid blockage design.

Presented as Paper 78-418 at the 3rd International Heat Pipe Conference, Palo Alto, Calif., May 22-24, 1978; submitted July 5, 1978; revision received Nov. 3, 1978.

Index categories: Heat Pipes; Spacecraft Temperature Control.

*Head, Energy Conversion & Heat Transfer Division. Member AIAA.

†Group Leader, Low Temperature Heat Pipes.

‡Staff Member, Energy Conversion & Heat Transfer Division.

§Staff Member, Thermal Control Section.

Table 1 Maximum capillary rise height, ammonia at 20°C ($\cos\theta = 0.7$)

Capillary structure	Rise height, mm
100 mesh screen	38.5
0.2 mm (triangular) grooves	25.2
0.6 mm (rectangular) grooves	8.4
0.7 mm (rectangular) grooves	7.1

Table 2 Reverse-mode heat flow in the wall

Material	k, W/cmK	Wall thickness, mm	Heat flow, W
Stainless steel	0.15	0.5	0.047
Aluminum	2.0	1	1.58

Table 3 Theoretical shutdown energy Q_{SD}

Concept	Axial grooves	Eight-shaped artery	Modular artery
Wall thickness, mm	1	0.5	0.5
$m_{l,\mathrm{ev+ad}}$, g	(4.5)	8.9	4.9
$m_{l,\mathrm{wick}}$, g	3.2	3.5	7.2
Q_{SD}, Wh			
Blockage	(1.5)	2.9	1.6
Trap	1.1	1.2	2.4

Table 4 Predicted maximum forward-mode performance, ammonia at 20°C ($\cos\theta = 0.7$)

Wick design type	o.d., mm	Maximum performance, W Horizontal orientation	Evaporator 5 mm high
Axial grooves			
0.6 mm wide, 1.0 mm deep, 23 grooves	10	162	68
0.7 mm wide, 1.2 mm deep, 19 grooves	10	210	65
Modular artery	10	1475	1370
Eight-shaped artery	7	150	140

Bendability is no serious constraint for all three designs. However, in the case of complex artery structures, e.g. modular artery with 4 or 5 webs, the bend radius has to be relatively large to avoid performance degradations.

The forward-mode performance of the axial-groove heat pipe is above the required value of 167 W at 20°C for horizontal orientation. The arterial designs, on the other hand, are by far overdesigned (Table 4). The 10 mm o.d. modular artery design is a standard design at IKE. A reduction in diameter, however, would result in additional manufacturing problems. The standard eight-shaped artery design, on the other hand, has a 7 mm o.d. Thus, a 7 mm o.d. all-stainless-steel eight-shaped artery diode employing the liquid-trap technique was looked at as a very attractive alternative to the all-aluminum 10 mm o.d. axial-groove diode employing the liquid-trap technique (Table 4). This is especially true for cryogenic temperature applications. The axial-groove liquid-trap design was ultimately selected for further investigation, because it meets all specifications, is simple and reliable, and sufficient experience is available. The arterial design was rejected mainly to avoid any problems associated with the restart from the shutdown condition, i.e., with the artery depleted.

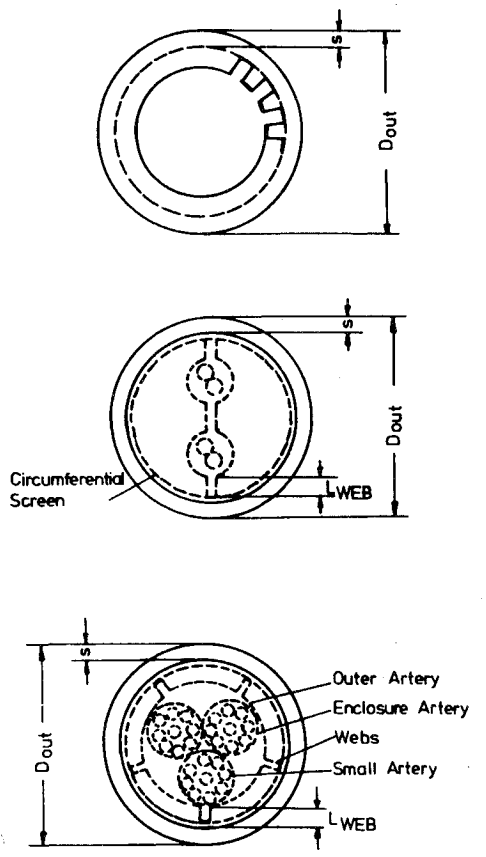

Fig. 1 Heat pipe cross section – axial grooves (top), eight-shaped artery (middle), modular artery (bottom).

Figure 2 shows the cross sections of heat pipe and liquid trap of the selected design. The wall material is hot-extruded aluminum alloy AlSiMg 0.5. The trap slab is made of 100-mesh aluminum screen which is reinforced by a perforated aluminum plate. The capillary structure at the trap wall consists of circumferential triangular grooves, 0.2 mm wide, 60 deg opening angle, 30 grooves/cm. The number of axial grooves in the heat pipe is 19.

Theoretical Analysis

Steady-State Performance

Forward-Mode Performance

The maximum performance as a function of tilt (evaporator above condenser) is depicted in Fig. 3 together with the respective experimental data. The forward-mode reference case is defined for horizontal operation and 20°C adiabatic temperature. The forward-mode conductance has been calculated to be $C_f = 11.0$ W/K. The heat-transfer coefficients for evaporation and condensation have been taken as $h_{\mathrm{ev}} = 0.70$ W/cm^{2}K and $h_{\mathrm{con}} = 1.36$ W/cm^{2}K, respectively.[9]

Reverse-Mode Performance

Shutdown of the diode is accomplished by cooling down the evaporator and trap from $20°\mathrm{C} + \Delta T_{\mathrm{ev}}$ to $-20°\mathrm{C} \pm 1$ K and simultaneously maintaining the condenser at a constant temperature of $+20°\mathrm{C} \pm 0.5$ K by means of an electrical heater.

For the completely shutdown diode with the condenser at 20°C and the evaporator and trap at −20°C, the reverse heat flow by thermal conduction in the wall was calculated to be $\dot{Q}_{\mathrm{rev}} = 1.14$ W. The respective reverse-mode conductance is $C_{\mathrm{rev}} = 0.0286$ W/K. Thus, the turndown ratio is $C_f / C_{\mathrm{rev}} = 384$.

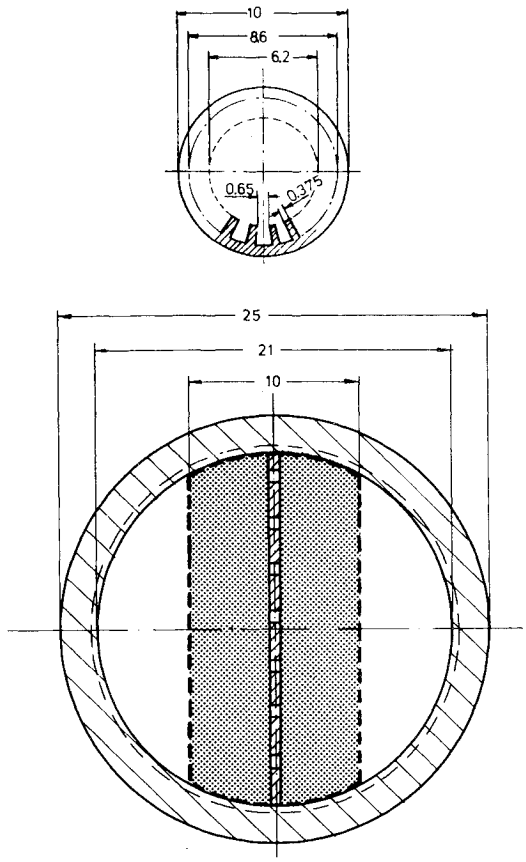

Fig. 2 Cross section of axial-groove heat pipe (top) and liquid trap with central slab (bottom) (all dimensions in mm).

Transient Shutdown

Theory

After initiation of shutdown, the evaporator and trap are rapidly cooled down. For the shutdown calculations, it is assumed that the sink temperature is decreasing in a step function. The energy to be removed from the diode is the sensible heat of evaporator and trap, $Q_{\text{sens, ev+tr}}$, and the sensible heat of the adiabatic section $Q_{\text{sens,ad}}$. $\dot{Q}_{\text{sens,ev+tr}}$, flows directly to the sink, whereas $\dot{Q}_{\text{sens,ad}}$ flows first through the diode by heat pipe action and thermal conduction and then to the sink. In addition, one has to account for the sensible heat of the evaporator and trap heater/calorimeter unit, $Q_{\text{sens,cal}}$. The respective heat flow goes directly to the sink. Since the diode heat pipe is shut down from the forward mode of operation, there will be a certain temperature gradient from evaporator (and trap) to condenser; i.e., the evaporator and condenser temperatures are somewhat above and below the adiabatic temperature. Therefore, immediately after initiation of shutdown, the heat pipe will continue to operate in the forward mode until the evaporator temperature T_{ev} has fallen below the condenser tempeature T_c, and $T_c > T_v$ (vapor temperature) $> T_{\text{ev}}$ (onset of shutdown). Since the thermal mass of the vapor is extremely small, any initial superheat of the vapor over the controlled condenser temperature would have a negligible influence on the shutdown behavior. However, concerning the initial superheat of the evaporator (and trap) as well as the adiabatic section, the respective sensible heat stored in these sections will delay the onset of shutdown to a certain degree. This time delay can be reduced linearly by reducing the forward-mode heat throughput. The time delay has not been accounted for in the shutdown calculations. After onset of shutdown, the heat flow in the diode is reversed. Liquid will be evaporated in the condenser, and the vapor will be condensed in the evaporator and trap. The fluid condensing in the trap will remain there; whereas

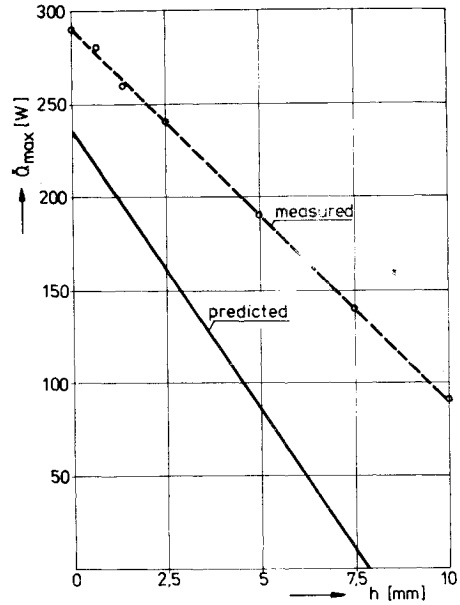

Fig. 3 Maximum performance of diode vs tilt height at 20°C.

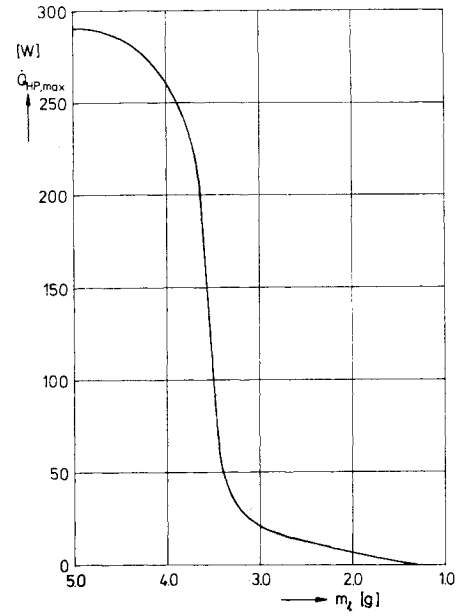

Fig. 4 Maximum performance of diode vs ammonia fill charge at 20°C and for horizontal orientation.

the fluid condensing in the evaporator will flow back to the condenser, be re-evaporated, and thus maintain the adverse heat pipe action. In addition, due to the adverse temperature gradient along the diode, there will also be a heat flow by thermal conduction from condenser to evaporator and trap.

The reverse heat flow would cause the condenser to fall in temperature below 20°C. This is prevented by electrical heat input to the condenser, $\dot{Q}_{\text{el}}$. The energy transferred through the diode during reverse-mode operation thus stems from the electrical heat input to the condenser and, to a smaller degree, from the sensible heat initially stored in the adiabatic section, $Q_{\text{sens,ad}}$. The sensible heat of the condenser, $Q_{\text{sens,cond}}$, has been neglected, since the condenser should essentially remain at a constant temperature of about 20°C. As described in the section on Experimental Results, this assumption turned out not to be valid at all, and it is planned to modify the theoretical model accordingly. After onset of shutdown, an adverse temperature gradient is developing along the heat pipe. With increasing temperature gradient the respective heat

flow by heat pipe action $\dot{Q}'_{HP} = C_f[T_c - T(t)]$, and by thermal conduction, $\dot{Q}_{cond} = C_{rev}/[T_c - T(t)]$, is increasing, too, until the maximum heat transport capability of the heat pipe, $\dot{Q}_{HP,max}$, is reached. $T(t)$ is the uniform temperature of evaporator and trap decreasing with time t, C_{rev} is the wall conductance, and $\dot{Q}_{HP,max}$ is a function of the liquid inventory m_l. The dependence of $\dot{Q}_{HP,max}$ on m_l has been determined experimentally for the investigated diode (see Fig. 4). Since m_l is decreasing with time, $\dot{Q}_{HP,max}$ will also decrease with time. The time corresponding to the intersection of curves $\dot{Q}'_{HP}$ and $\dot{Q}_{HP,max}$ has been designated t_{DO}, time for beginning of heat pipe dryout. The determination of t_{DO} is described later. The transient shutdown can thus be divided into two sections: one for $0 \le t \le t_{DO}$, the other for $t > t_{DO}$. Once $\dot{Q}_{HP,max}(t)$ and $T(t)$ are known, the complete shutdown power curve, i.e., $\dot{Q}'_{HP}(t)$ for $0 \le t \le t_{DO}$ and $\dot{Q}_{HP,max}(t)$ for $t > t_{DO}$, respectively, can be determined. For calculation of the transient shutdown power curve, a simple mathematical thermal model has been used.

A heat flow balance for node T ($T \equiv$ evaporator and trap temperature, also, adiabatic temperature) yields

$$\dot{Q}_s = \dot{Q}_{sens,ev+tr} + \dot{Q}_{sens,cal} + \dot{Q}_{sens,ad} + \dot{Q}_{HP} + \dot{Q}_{cond} \tag{1}$$

The various heat flows are

$$\dot{Q}_s = hA_s(T_s - T)$$

$$\dot{Q}_{sens,ev+tr} = -\frac{dT}{dt}(CM)$$

$$\dot{Q}_{sens,cal} = -\frac{dT}{dt}(CM)_{cal}$$

$$\dot{Q}_{sens,ad} = -\frac{1}{2}\frac{dT}{dt}(CM)_{ad}$$

$$\dot{Q}_{HP} = \begin{cases} C_f(T_c - T) & \text{for} \quad 0 \le t \le t_{DO} \quad (2a) \\ \dot{Q}_{HP,max}(t) & \text{for} \quad t > t_{DO} \quad (2b) \end{cases}$$

$$\dot{Q}_{cond} = C_{rev}(T_c - T)$$

where h is the overall heat-transfer coefficient between evaporator/trap and sink (see section on Numerical Results), A_s is the respective heat transfer area, T_s is the sink temperature, (CM) is the thermal mass of evaporator and trap, $(CM)_{cal}$ is the thermal mass of evaporator heater/calorimeter unit, and $(CM)_{ad}$ is the thermal mass of adiabatic section.

For the time period $0 \le t \le t_{DO}$, the heat flow balance [Eq. (1)] can be rewritten

$$\frac{dT}{dt} + \frac{B}{A}T - \frac{C}{A} = 0 \tag{3}$$

with

$$A \equiv (CM) + (CM)_{cal} + \tfrac{1}{2}(CM)_{ad}$$

$$B \equiv hA_s + C_f + C_{rev}$$

$$C \equiv hA_sT_s + T_c(C_f + C_{rev})$$

The initial conditions are

$$T = T_c = 293 \text{ K} \qquad \text{for } t = 0$$

$$T_s = 293 \text{ K} \qquad \text{for } t = 0$$

$$T_s = 253 \text{ K} \qquad \text{for } t > 0$$

The differential equation (3) can be solved analytically by

$$T(t) = \frac{C}{B} + \left(T_c - \frac{C}{B}\right)\exp\left(-\frac{B}{A}t\right) \tag{4}$$

The reverse-mode heat flow by heat pipe action, $\dot{Q}_{HP}(t)$, can now be determined using Eqs. (2a) and (4).

For the time period $t \ge t_{DO}$, it has been assumed that the heat flow by thermal conduction has already reached its steady-state value, $\dot{Q}_{cond,\infty} = C_{rev}(T_c - T_\infty)$. The steady-state value is calculated by setting $T_\infty = T_s = 253$ K. This assumption includes another minor error since T cannot quite reach T_s, due to the small but finite steady-state heat flow by thermal conduction. With the preceding assumptions, $\dot{Q}_{HP,max}(t)$ becomes independent of temperature $T(t)$ and is only a function of the liquid inventory $m_l(t)$. Since $\dot{Q}_{HP,max}$ has been experimentally determined as a function of m_l (Fig. 4), the determination of the transient behavior of $\dot{Q}_{HP,max}$ is reduced to the calculation of the transient behavior of m_l. This relation $\dot{Q}_{HP,max}(t) = f[m_l(t)]$ is established according to the following procedure:

$$m_l(t) = m_{tot} - m_{trap}(t) = m_{tot} - \int_{t=0}^{t} \dot{m}_{trap}\,dt$$

where $m_l(t)$ is the actual liquid inventory in heat pipe at time t; m_{tot} is the total initial liquid inventory in the heat pipe; $m_{trap}(t)$ is the amount of liquid trapped in trap at time t, and

$$\dot{m}_{trap}(t) = a(\dot{Q}_{HP}(t)/h_{fg})$$

a is the factor defining the fraction of condensed fluid which is trapped in the trap (see section on Numerical Results), and h_{fg} is the latent heat of vaporization of working fluid.

Thus,

$$m_l(t) = m_{tot} - \frac{a}{h_{fg}}\int_{t=0}^{t} \dot{Q}_{HP}(t)\,dt \tag{5}$$

The integral between $t = 0$ and t can be split into two integrals, the first between $t = 0$ and $t = t_{DO}$ and the second between $t = t_{DO}$ and t. The first integral can be solved analytically. This leads to an expression for the amount of liquid trapped in the trap during the time interval $0 \le t \le t_{DO}$:

$$m_{DO} = \frac{a}{h_{fg}}\int_{t=0}^{t_{DO}} \dot{Q}_{HP}(t)\,dt$$

with $\dot{Q}_{HP}(t)$ from Eq. (2a).

Thus,

$$m_l(t) = m_{tot} - m_{DO} - \frac{a}{h_{fg}}\int_{t=t_{DO}}^{t} \dot{Q}_{HP}(t)dt \tag{6}$$

with $\dot{Q}_{HP}(t)$ from Eq. (2b).

The reverse-mode heat flow by heat pipe action can now be determined using Eq. (6) together with Fig. 4. For the iterative numerical solution of the problem, the curve in Fig. 4 is represented by $\dot{Q}_{HP,max}$ values for 36 m_l values. A cubic interpolation is used within the m_l intervals. For the first time interval following time t_{DO}, the value $\dot{Q}_{HP,max}$ (t_{DO}) at the intersection of $\dot{Q}'_{HP}(t)$ and $\dot{Q}_{HP,max}(t)$ is used as a starting value. Using Eq. (6) and Fig. 4, a new value $\dot{Q}_{HP,max}$ at time $t_{DO} + \Delta t$ is calculated. This value is improved by an iteration procedure. At any time t_i this iteration procedure is terminated when

$$\dot{Q}_{HP,max,i}(\text{old}) - \dot{Q}_{HP,max,i}(\text{new})/\dot{Q}_{HP,max,i}(\text{new}) \le \epsilon$$

The iteration for the next interval Δt at time t_{i+1} is started with $\dot{Q}_{HP,max,i}$ (new), etc.

For determination of time t_{DO}, the intersection of curves $\dot{Q}'_{HP}(t)$ and $\dot{Q}_{HP,max}(t)$ has to be calculated. $\dot{Q}'_{HP}(t)$ is known from Eqs. (2a) and (4) with t not limited to t_{DO}. $\dot{Q}_{HP,max}(t)$ is determined by simultaneously using Eq. (5) with Eq. (2b) and Fig. 4.

Numerical Results

The theoretical model comprises two critical input data: one is the overall heat-transfer coefficient between evaporator/trap and sink, h, which cannot be calculated precisely. A rough estimate resulted in h being of the order of 0.1 W/cm^{2}K. This heat-transfer coefficient was adjusted to experimental results in such a way that the numerically calculated cool-down curve of the evaporator and trap temperature agreed with experimental results. The value of h found by this adjustment was 0.13 W/cm^{2}K.

The parameter a, defining the condensation rate in the trap, also cannot be precisely calculated. An upper limit was calculated based on the assumption that for isothermal evaporator and trap walls the condensation rates in evaporator and trap are determined by the respective surface areas. This upper limit is 0.69. The vapor flow from diode into trap is influenced by an orifice plate at the end of the evaporator and by the thick slab of the trap. For numerical calculations, a factor of $a=0.3$ has, therefore, been chosen which accounts for the strong restriction of the vapor flow by orifice end plate and trap slab. The theoretical upper limit could only be approached if the vapor flow were completely nonrestricted.

In Fig. 5, the transient shutdown power curve, $\dot{Q}_{rev}(t)$, is depicted for three different cases: 1) no limitation exists for the heat input to the condenser; i.e., the condenser heater can provide enough power so that the heat pipe can operate up to its maximum heat-transfer capability; 2) the heat input to the condenser is limited to 110 W; and 3) the heat input is limited to 63 W. Cases 2) and 3) reflect the experimental conditions defined by the used controller for the condenser heater.

Figure 6 shows the transient shutdown energy curves, $Q_{SD}(t)$, for the same three cases. These curves have been directly derived from Fig. 6, making use of the relation

$$Q_{SD}(t) = \int_{t=0}^{t} \dot{Q}_{rev}(t)\,dt$$

The shutdown power curves reach an asymptotic value ($d\dot{Q}_{rev}/dt = 0$) after about 20 min, the time for complete shutdown of the diode. Accordingly, the shutdown energy curves reach an asymptotic slope ($d^2Q_{SD}/dt^2 = 0$) after about 20 min. Shutdown energy for all three cases was determined to be approximately 13,300 Ws = 3.69 Wh, with 20 min taken as shutdown time.

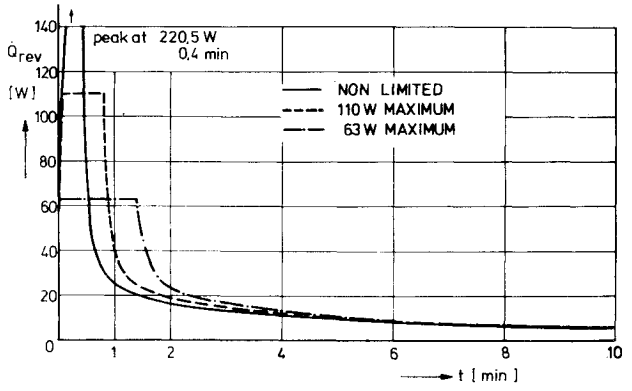

Fig. 5 Transient shutdown power.

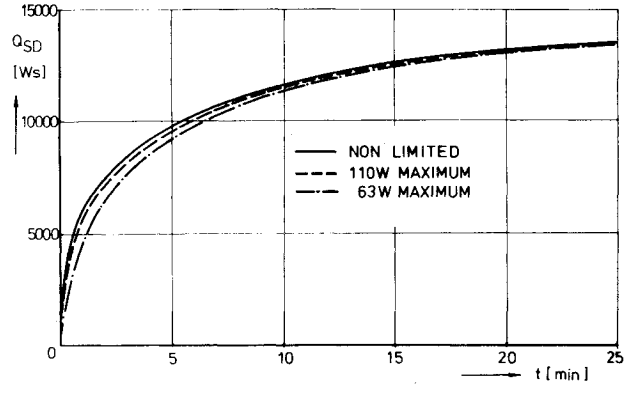

Fig. 6 Transient shutdown energy for the three cases shown in Fig. 5.

Test Setup and Instrumentation

A schematic of the test setup is shown in Fig. 7. The instrumentation varies slightly for the different modes of operation.

During performance measurements in the forward mode, the diode is instrumented with a heater element and a condenser block, clamped directly on the diode surface. The 100-mm long heater element is a combined heating/cooling device consisting essentially of two copper half-shells into which both coax heater wires and coolant tubes are integrated. The heat input to the diode evaporator section is maintained by electrical resistance heating of the heater wires using a stabilized dc source. The heat load is measured by a voltmeter and an ammeter. The evaporator/trap coolant loop is empty and the respective cryostat (see Fig. 7) is not operating. The heat transported in the diode is removed by the condenser coolant flowing through cooling channels within both halves of the condenser block, which are bolted together and fitting tightly on the diode surface. The temperature of the coolant

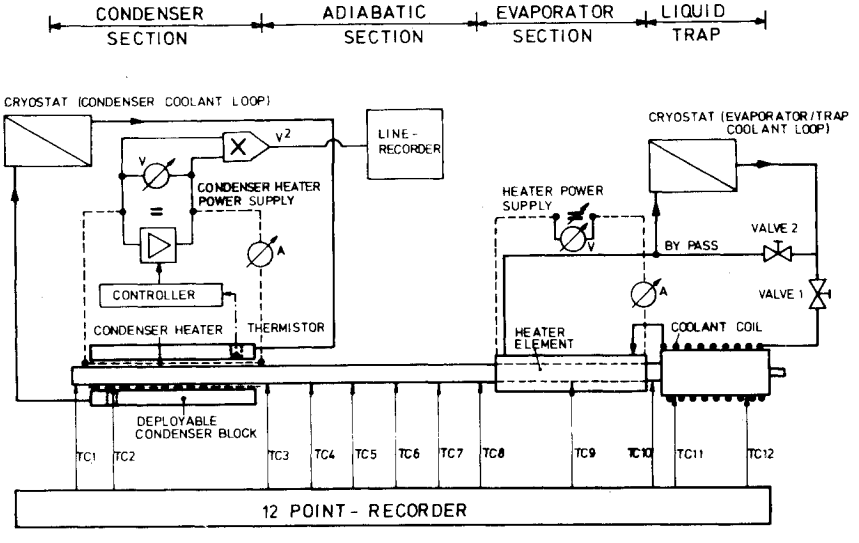

Fig. 7 Schematic of test setup without thermal insulation.

and, accordingly, the temperature of the diode can be adjusted by the condenser cryostat.

For shutdown tests a deployable condenser block is used, which has to be removed from the diode condenser section at initiation of shutdown. Beneath the deployable condenser block an electrical resistance heater made from nichrome ribbon is wrapped around the pipe between two layers of Kapton foil along the 100-mm long condenser section of the diode. This heater is used to maintain the condenser section at a constant temperature of $T^* = 20°C \pm 0.5$ K throughout the shutdown period and is controlled via a thermistor by a proportional controller. The thermistor housing is epoxy-bonded to the diode surface and both the thermistor leads and the thermocouple wires of TC2 (see Fig. 7) are guided through respective holes in the condenser block. In addition to the a/m instrumentation, the coolant channels of the combined heating/cooling device clamped to the diode evaporator section, and a separate cooling device for the trap consisting of a slotted copper tube with coolant channels, are used for this test.

Prior to shutdown the diode is operated in the forward mode with a heat load of 10 W to insure that any liquid is in the heat pipe section of the diode. At initiation of shutdown, the deployable condenser block is removed from the diode surface; i.e., the condenser block halves are separated by spring tension sliding along fitting pins. Between the removed condenser block halves and the diode condenser section there is a gap of about a 5-mm width, and a separate support prevents the blocks from touching the diode. The deployed condenser block acts as a guard heater, as its temperature is maintained at about 20°C by means of the condenser coolant loop. Simultaneously, at initiation of shutdown, the condenser heater is actuated, valve no. 1 is opened, and valve no. 2 is closed (see Fig. 7). Thereby, the evaporator coolant of temperature −20°C, which has been flowing through a bypass, now starts to cool down the trap and the evaporator section very rapidly. During the shutdown period, the actual heat input to the condenser heater needed to maintain temperature T^* at a constant value of $20°C \pm 0.5$ K is continuously recorded using an electronic multiplier for the actual voltage as the measured quantity.

For restart tests, an additional heater is mounted on the trap which is controlled by a temperature difference controller

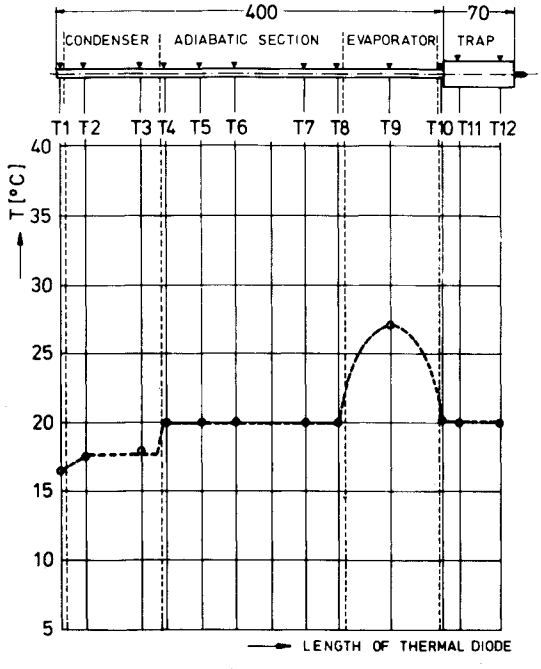

Fig. 8 Axial temperature distribution for power of 100 W and horizontal orientation.

to maintain the trap at a temperature about 1 K above the temperature of the evaporator section of the diode at any time. During these tests the fixed condenser block has to be employed again to insure sufficient heat removal from the diode with a tolerable temperature difference between coolant and condenser section.

The temperature distribution along the diode is measured by means of twelve thermocouples which are epoxy-bonded to the diode surface. The location of the thermocouples is indicated in Fig. 7. During all the tests, the diode is well insulated using Armaflex insulation and the evaporator section is additionally surrounded by some layers of Fiberfrax. The diode is mounted, using three supports, on an optical bench, which can be tilted to all necessary positions.

Experimental Results and Comparison with Theoretical Predictions

Steady-State Forward-Mode Performance

Extended experiments have been carried out with a development model of the diode. The maximum heat transport capability $\dot{Q}_{max}$ as a function of tilt height (evaporator above condenser) is depicted in Fig. 3 together with the respective theoretical results. The measured capability is much better than the predictions. For horizontal orientation and small tilt heights, this can be explained by the conservative assumption of $\cos\theta = 0.7$. The discrepancy between theory and experiment is larger at high tilts. This can be explained by the fact that when approaching $\dot{Q}_{max}$ the upper grooves of the heat pipe will deplete and the excess liquid will form a puddle at the condenser end. Therefore, especially at higher tilt heights, both the effective tilt height and the effective length of the heat pipe are reduced and, consequently, higher performances can be achieved.

The forward-mode conductance has been determined from the axial temperature distribution along the diode (Fig. 8). Thermocouples at both ends of the evaporator section showed the same temperature as the adiabatic section. A thermocouple in the middle of the evaporator was located between two windings of the nichrome ribbon heater, and showed a considerably higher temperature. It was felt, therefore, that an average evaporator temperature could not be appropriately defined. To derive the forward-mode conductance for the whole diode, the same ratio of the heat-transfer coefficients for evaporation and condensation, respectively, as determined for the ATS-6 axial groove/ammonia heat pipes, has been used.[9] Thus, for horizontal operation of the diode at 20°C adiabatic temperature and heat throughputs of 100 and 200 W, respectively, a forward-mode conductance of 13.8 W/K was found. This value agrees well with the predicted figures of 11.0 W/K.

Transient Shutdown and Steady-State Reverse-Mode Performance

Shutdown tests have been carried out according to the following procedure. Prior to shutdown the diode is operated in the forward mode with a heat load of 10 W and, in addition, the trap is heated to a temperature 20 K above the adiabatic temperature of the diode to insure that no liquid is in the trap. At initiation of shutdown, the following activities are carried out simultaneously: 1) mark initiation of shutdown on both line-recorder ($\dot{Q}_{rev}$ vs time) and 12-point recorder (temperature vs time); 2) turn off evaporator heater power; 3 s) switch on controller power supply, that is, actuate condenser heater; 4) decouple condenser block from condenser section of the diode (in a time period less than 3 s); and 5) open valve of coolant loop to cool down trap and evaporator section of the diode to a temperature of −20°C.

Figures 9 and 10 show two transient shutdown power curves with the maximum heat input to the condenser as parameter, viz., 63 W and 110 W. The plateau for 63 W heat input is maintained for 121 s, as compared to 65 s for the 110 W case.

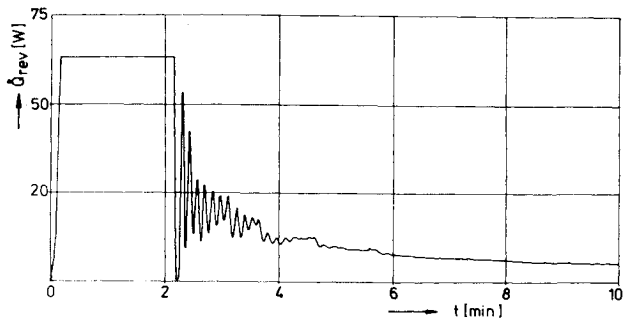

Fig. 9 Transient shutdown power for 63 W maximum heat input to condenser.

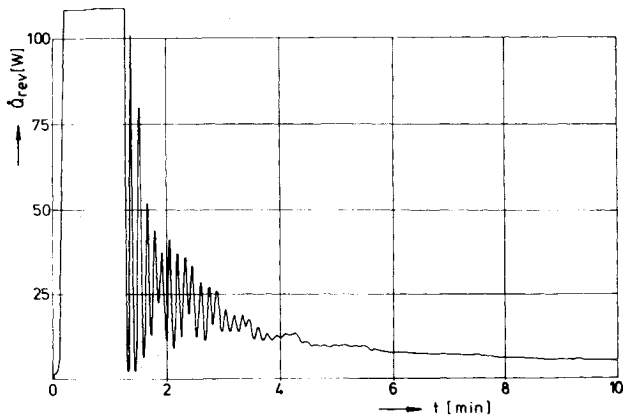

Fig. 10 Transient shutdown power for 110 W maximum heat input to condenser.

The spikes of the curves are not results of heat pipe operation, but they are caused by the time constant of the controller. It can be seen that steady-state conditions, i.e., constant heat input to the condenser, are achieved after approximately 20 min for both cases. The respective steady-state reverse-mode heat flow has been measured to be approximately the same for both cases, that is, 1.5 W. This amount of heat flows for a temperature difference of about 34 K maintained along the adiabatic section. Therefore, the reverse-mode conductance is 0.0449 W/K and the turndown ratio is 308. These steady-state figures are in good agreement with predictions.

Figure 11 shows the transient axial temperature profiles along the diode for the 110 W case. Here, too, it can be seen that a steady-state condition, i.e., a linear temperature decrease from condenser to evaporator, is established after approximately 20 min. This agrees well with the results obtained from the transient shutdown power curves, and also with the individual transient diode temperatures.

Figure 12 shows the transient behavior of the shutdown energy, $Q_{SD} = \int_{t=0}^{t} \dot{Q}_{rev}(t)\,dt$, for the same two shutdown tests discussed previously. The shutdown energy curves shown are directly derived from Figs. 9 and 10. As indicated in Fig. 11, especially during the first moments of shutdown, the far condenser end gets considerably overheated, due to the instrumentation used. To maintain the thermistor which is controlling the condenser temperature at $T^* = 20°C \pm 0.5$ K, a high heat input to the condenser is required. The essentially uniformly wrapped nichrome ribbon heater will cause a temperature profile along the condenser. In addition, the condenser will rapidly dry out from its far end. When the condenser is above room temperature, it will be cooled by convection and radiation. These heat losses have to be subtracted from the measured shutdown power and a respective correction has to be made for the shutdown energy. The shutdown energy curves reach an asymptotic slope at about 20 min, which is equivalent to the fact that the shutdown power

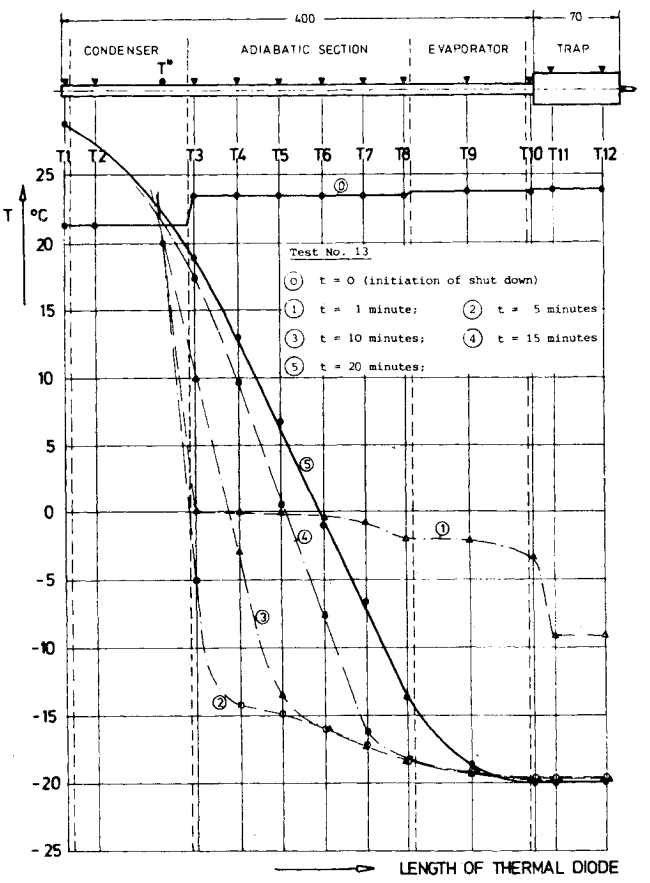

Fig. 11 Transient axial temperature profiles during shutdown for 110 W maximum heat input to condenser.

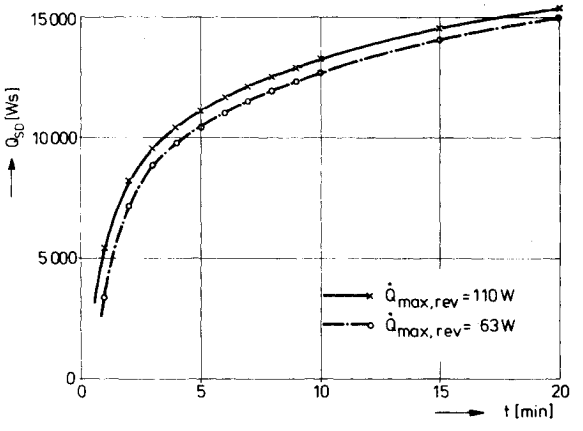

Fig. 12 Transient shutdown energy for the two cases shown in Figs. 9 and 10.

curves reach a horizontal asymptote after the same time. The shutdown energy curve for the 110 W case is above the curve for the 63 W case. The shutdown energies at 20 min, i.e., after complete shutdown, are 15,470 and 14,980 Ws, respectively. If the losses to the surroundings are accounted for, this difference essentially disappears. Then the estimated shutdown energies are about 14,470 Ws = 4.02 Wh for the 110 W case and 14,310 Ws = 3.98 Wh for the 63 W case. These data agree reasonably well with theoretical predictions. However, they are by a factor of 2.5 above the minimum theoretical shutdown energy, viz., the latent heat of the liquid inventory of the diode (1.58 Wh). This indicates that there is a certain backflow by heat piping action during reversal.

The time for complete shutdown could be reasonably well determined to be about 20 min. However, applications are

Table 5 Comparison between theoretical predictions and experimental results with diode development model (rounded figures have been used)

	Theory		Experiments	
Maximum forward-mode performance, W, at 20°C and horizontal orientation	230		290	
Forward-mode conductance C_f, W/K	11.0		13.8	
Reverse-mode heat flow, W	1.1		1.5	
Reverse-mode conductance C_{rev}, W/K	0.029		0.045	
Turndown ratio, C_f / C_{rev}	380		310	
Minimum shutdown energy, Wh $Q_{SD,min} = m_l h_{fg}$	1.6		...	
Shutdown energy, Wh	$Q_{SD}(t_{SD})$[a]	$Q_{SD}(t^+_{SD})$[b]	$Q_{SD}(t_{SD})$	$Q_{SD}(t^+_{SD})$
$\dot{Q}_{rev,max} = 63$ W	3.7	3.3	4.0	3.6
$\dot{Q}_{rev,max} = 110$ W	3.7	3.3	4.0	3.6
$\dot{Q}_{rev,max}$ – not limited	3.7	3.3	–	–
Shutdown time, min	t_{SD}	t^+_{SD}	t_{SD}	t^+_{SD}
$\dot{Q}_{rev,max} = 63$ W	~20	~12.3	~20	~13.3
$\dot{Q}_{rev,max} = 110$ W	~20	~11.8	~20	~12.9
$\dot{Q}_{rev,max}$ – not limited	~20	~11.2	...	...

[a] t_{SD} is the time for complete shutdown; i.e., $d\dot{Q}_{rev}(t)/dt = 0$, $d^2 Q_{SD}(t)/dt^2 = 0$.
[b] t^+_{SD} is the effective shutdown time for $Q_{SD} = 0.9\, Q_{SD}(t_{SD})$.

conceivable where a somewhat higher reverse heat flow than by thermal conduction can be tolerated or where diode operation is essentially used for switching purposes, and fast switching cycles are interesting. Then a shorter effective shutdown time could be defined. Another reason for defining a shutdown time smaller than the one for complete shutdown is because of the fact that, when approaching asymptotic values of shutdown power or shutdown energy, the precision for determining the associated shutdown times gets worse. As an effective shutdown time, t^+_{SD} has been tentatively chosen. t^+_{SD} is the time when $Q_{SD}(t)$ has reached 90% of $Q_{SD}(t_{SD})$. The respective data have been included in Table 5 where the comparison between theory and experiments is summed up.

The restart of the diode has been experimentally investigated. Prior to tests, the trap was cooled by means of a separate coolant loop to a temperature of about 0°C for 1/2 h to insure that any liquid is in the trap. Then the temperature controller was switched on and the trap heater was actuated. After about 80 s the trap temperatures were equal to the evaporator temperatures. This situation was defined as initiation of restart. A heat input of 10 W was then applied to the evaporator section while the coolant flow through the condenser block was maintained at 20°C. The heat load of 10 W resulted in a temperature increase of the evaporator section of 5 K above the adiabatic temperature, but it recovered after 3 min. Five minutes after initiation of restart the heat load was increased from 10 to 50 W and after another 5 min to 100 W. No overshoot in temperatures could be detected.

The restart test was repeated reducing the time period for switching from 10 W to 50 W to 2 min after initiation of restart. This time there was a temperature overshoot of 20 K of the evaporator above the adiabatic section, but it recovered again 3.5 min after initiation of restart, i.e. 1.5 min after the power step. There was no overshoot when the heat load was increased from 50 to 100 W after another 5 min.

Summary

The developed axial-groove all-aluminum liquid-trap diode is of simple design and reveals both good forward-mode and shutdown characteristics. Extended testing with the diode development model under different thermal boundary conditions demonstrated the diode's reliable shutdown and restart behavior. Experiments with two improved prototype diodes are presently in progress.

A theoretical model has been developed which adequately describes the transient shutdown of the diode. Agreement with experiment is good. Still, the theory needs further improvement, especially with respect to a better understanding of the condensation phenomena in the evaporator and trap during reverse-mode operation. To a lesser degree, this also holds for the evaporation process in the reverse mode of operation when the fluid inventory is steadily decreasing.

Acknowledgment

This research was supported under Contract No. 2993/76/NL/PP(SC) from European Space Research and Technology Centre, Noordwijk, The Netherlands.

References

[1] Swerdling, B. and Kosson, R., "Design, Fabrication and Testing of a Thermal Diode," NASA CR-114 526, Nov. 1972.

[2] Kosson, R.L., Quadrini, J.A., and Kirkpatrick, J.P., "Development of a Blocking Orifice Thermal Diode Heat Pipe," AIAA Paper 74-754, AIAA/ASME Thermophysics and Heat Transfer Conference, Boston, Mass., July 1974.

[3] Quadrini, J. and Kosson, R., "Design, Fabrication and Testing of a Cryogenic Thermal Diode," NASA CR 137 616, Dec. 1974.

[4] Brennan, P.J. and Groll, M., "Application of Axial Grooves to Cryogenic Variable Conductance Heat Pipe Technology," *Proceedings of the 2nd International Heat Pipe Conference,* Bologna, Italy, March/April 1976.

[5] Basiulis, A., "Unidirectional Heat Pipes to Control TWT Temperature in Synchronous Orbit," Symposium on Thermodynamics and Thermophysics of Space Flight, Palo Alto, Calif., March 1970.

[6] Brost, O. and Schubert, K.P., "Development of Alkali-Metal Heat Pipes as Thermal Switches," *Proceedings of the 1st Interntional Heat Pipe Conference,* Stuttgart, Federal Republic of Germany, Oct. 1973.

[7] Sun, T.H. and Prager, R.C., "Development of a Switchable Cryogenic Heat Pipe for Infrared Detector Cooling," AIAA Paper 74-751, AIAA/ASME Thermophysics and Heat Transfer Conference, Boston, Mass., July 1974.

[8] Quadrini, J.A. and McCreight, C.R., "Development of a Thermal Diode Heat Pipe for Cryogenic Applications," AIAA Paper 77-192, AIAA 15th Aerospace Sciences Meeting, Los Angeles, Calif., Jan. 1977.

[9] Schlitt, K.R., Brennan, P.J., and Kirkpatrick, J.P., "Parametric Performance of Extruded Axial Grooved Heat Pipes from 100 to 300°K," AIAA Paper 74-724, AIAA/ASME Thermophysics and Heat Transfer Conference, Boston, Mass., July 1974.